REPORT DOCUMENTATION PAGE

AFRL-SR-BL-TR-01-

0572

1. REPORT DATE (DD-MM-YYYY)	2. REPORT TYPE	3. DATES COVERED (From - To)
10-3-01	Final	3-1-99 to 11-30-00

4. TITLE AND SUBTITLE

Quantitative Characterization of Fretting Damage in Aircraft Turbine Disks

5a. CONTRACT NUMBER

5b. GRANT NUMBER

F49620-99-1-0148

5c. PROGRAM ELEMENT NUMBER

5d. PROJECT NUMBER

5e. TASK NUMBER

5f. WORK UNIT NUMBER

6. AUTHOR(S)

Joseph N. Gray, Lalita Udpa, Feyzi Inanc

7. PERFORMING ORGANIZATION NAME(S) AND ADDRESS(ES)

Iowa State University
Office of Sponsored Programs Administration
Rm 15 Pearson
Ames, IA 50011-2207

9. SPONSORING/MONITORING AGENCY NAME(S) AND ADDRESS(ES)

ONRRO Chicago
536 South Clark St., Rm 208
Chicago, IL 60605-1588

AFOSR/NA
801 N. Randolph St. Rm 732
Arlington, VA 22203-1977

10. SPONSOR/MONITOR'S ACRONYM(S)

ONRR AFOSR

11. SPONSOR/MONITOR'S REPORT NUMBER(S)

12. DISTRIBUTION/AVAILABILITY STATEMENT

Unlimited

Approved for public release; distribution unlimited.

13. SUPPLEMENTARY NOTES

14. ABSTRACT

A feasibility study was completed to evaluate a low cost, robust optical inspection method for detecting and characterizing fretting damage on metal surfaces. The effects of the quality and type of the light illumination and the angle of the illumination were measured. Dark field and light field imaging were used to generate images to measure the size of fretting areas. A signal dependence upon the depth of the surface roughness and the illumination angle was demonstrated. The artifacts introduced by the camera image acquisition system were found to be important to successful image processing and means were developed to remove them. Image processing methods based on morphological operations were developed to determine the fretting region of interest in the image. The study demonstrated a method of fretting surface characterization.

15. SUBJECT TERMS

Keywords: fretting, morphological image processing, specular reflection, CCD camera

16. SECURITY CLASSIFICATION OF:			17. LIMITATION OF ABSTRACT	18. NUMBER OF PAGES	19a. NAME OF RESPONSIBLE PERSON
a. REPORT	b. ABSTRACT	c. THIS PAGE	UU	18	Joseph N. Gray
					19b. TELEPHONE NUMBER (Include area code) 515-294-9745

Quantitative Characterization of Fretting Damage in Aircraft Turbine Disks
Final Report

Introduction

The principle goal of this project was to demonstrate effective methods of acquiring optical image data of surfaces with the potential to be deployed in the field and to demonstrate a data analysis method suitable for extraction from the images signatures for determining the spatial dimensions and depth of surface features. We have developed both a data acquisition method and image signature extraction tools the show promise in being extended to develop a prototype instrument.

Background

The present methods for detecting fretting damage in turbine disks involve a visual inspection using hand mirror to access the loaded surfaces of a turbine disk fir tree. The roughness of the fretting surface is determined using the visual information and supplementing it with tactile information obtained by running a finger across the surface. A categorization of the damage into light, moderate and severe is made with disks having severe damage levels being rejected from service. The requirement that any NDE method being considered must have the potential for automated implementation in RFC facility at the ALC's brings a number of fundamental key problems to light requiring solution. The automated detection and characterization involves a combination of texture analysis (rough surfaces) and feature extraction (ridge detection). Developing signatures for use in an expert system (neural net based) requires a good set of representative samples and adequate image quality. The small features (~1-3 mils) of fretting damage and the difficult access of the damaged surface present imaging challenges.

Fretting damage is a result of two highly loaded surfaces rubbing together (1). This rubbing action can cause a removal of the thin oxide layer typically covering the surfaces of metals revealing small areas of bare metal which, in turn, can result in micro-bonding of these metal surfaces and subsequent tearing of those small bonded areas. The repetition of these events results in metal and oxides building up in furrows. (see figure 1). The observed furrows in the fir tree region of turbine disks have been reported to be 1 -3 mil range in height and 10 -15 mils in length with a few tens of mils separation between furrows. As noted earlier, one of the deleterious consequences of these small shifts of material is a significant lost of fatigue life in that cracks begin to grow from these regions much sooner than for a typical smooth surface. To implement a means to detect and characterize fretting, two elements must be

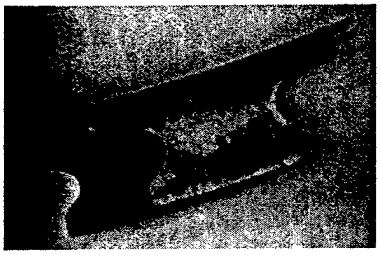

Figure 1a

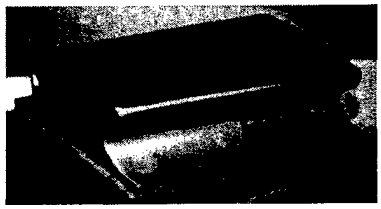

Figure 1b

Figure 1c

Figure 1 Two views of a section of a turbine disk with fretting damage. Figure 1a is an end view of the disk, Figure 1b is a side view. Figure 1c is an example of a crack initiated from fretting damage.

present, first an understanding of the effect of fretting on the remaining fatigue life of the material, in other words, an effects of damage, and, secondly, the development of an NDE method with sufficient dynamic range and sensitivity to quantitatively characterize the fretting damage. It is the second point that is the focus of the work reported here.

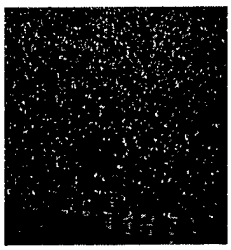

Figure 2a

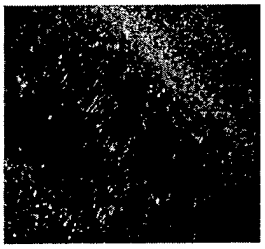

Figure2b

Figure 2c

Figure 2 Optical micrographs of the turbine disk section shown in figure 1. Figure 1a is a normal region without fretting. The ruler shows millimeter spacing. Figure 2b shows the ridge form of fretting. Each ridge is 0.1 mm wide; the fretting surface is 3 mm wide. Figure 2c show the texture form of fretting.

Several samples of the artificial fretting and examples of actual fretted turbine disks were acquired from Dr. Crane at Wright Patterson Materials Laboratory.

In this work we evaluated two optical methods of nondestructively quantifying the surface morphological changes that occur as a result of fretting. The evaluation of the techniques focused on demonstrating sufficient signal to noise (SNR) capabilities, scanning speeds, cost and/or time constraints, size constraints since the transducer or detector must fit into the "fir tree" of the engine disk. There were two distinct technical issues that need to be solved, first obtaining an adequate signal in a restricted geometry and, second, developing signatures from those signals that can be used to characterize the fretting.

Results

Image Acquisition System

An image acquisition system has been developed with two important design parameters in mind. One of these was to have a small imaging system that can reach into small openings of a turbine disk. This was an issue imposed by the nature of the problem, namely that the fretting typically takes place on the inner surface of the disk fir tree. Imaging this location through conventional cameras is quite difficult because of the camera and lens sizes. The other issue that played important role in the image acquisition system was to obtain an image that had minimal background light intensity gradients. Any light source that can be used in such a cramped location is likely to have a very small spot size. Therefore, the light intensity will fall off rapidly with distance from the focus point. This imposes a two dimensional gradient on the background light intensity. The main input for the image processing algorithms is the gray levels provided by the imaging system. Nonuniformity in background levels poses increasing difficulty in processing the images to obtain the signal for flaw characterization.

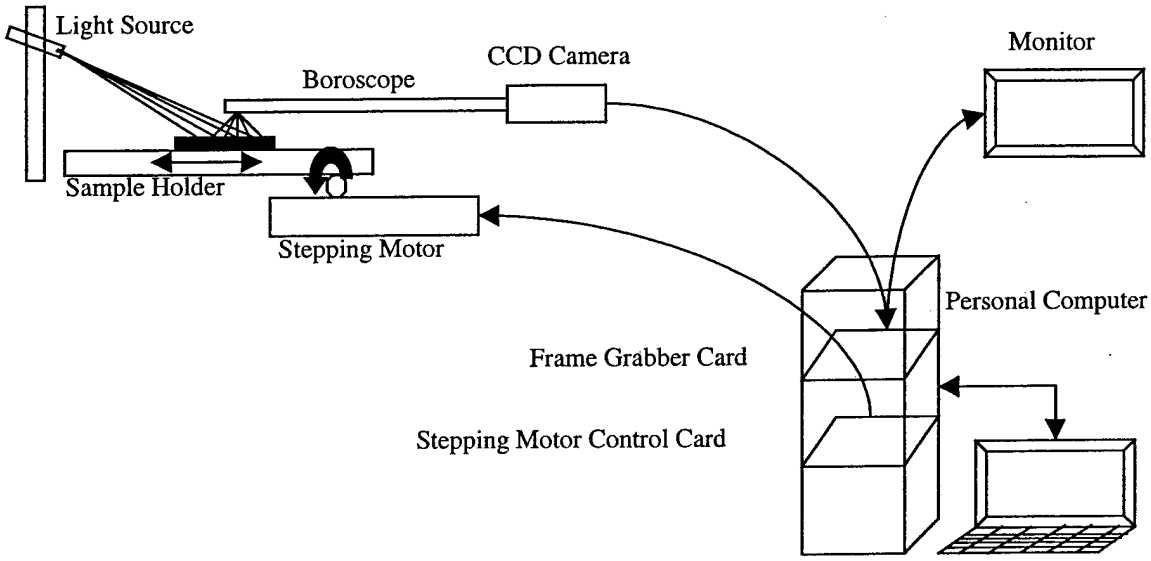

Figure 3 shows a block diagram of the image acquisition system.

The system, shown in figure 3, is made up of a personal computer with a 640x480, 8 bit frame grabber and a stepping motor control card. The CCD camera is connected to a boroscope 450 mm in length and 7 mm diameter. It is used to both illuminate the target and transmit image back to the eyepiece. For our system, the eyepiece is mounted on the CCD camera, which has a pixel size of 20 microns. The stepping motor used is capable of moving the platform with increments of 0.8 microns.

We developed a custom data acquisition program for running the image system. The user interface for that software is shown in Figure 4. The software can store the acquired images in both ASCII and bitmap formats for further analysis. The parameters

set through the software include the number of step increments for each line, number of total lines for an image, number of frames integrated per line, number of overall images to be taken and line number to be used from two dimensional images.

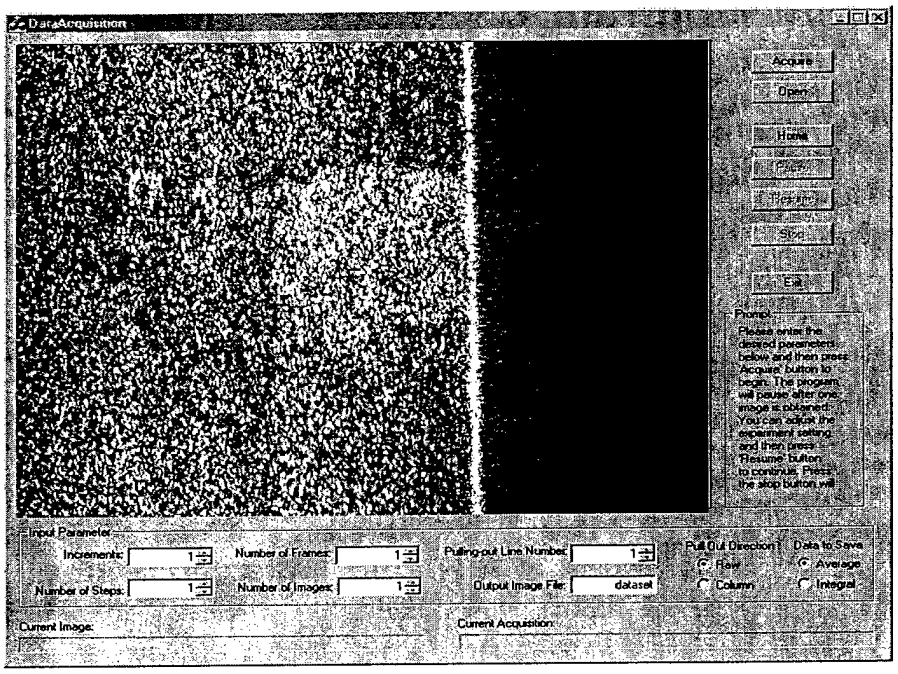

Figure 4. Interface for the data acquisition program controlling the sample scanning and image collection. The image shown is from a laser illumination of a sample.

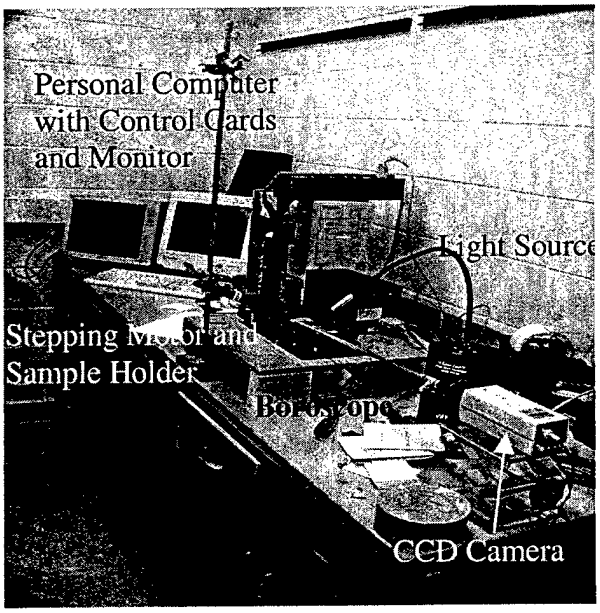

Figure 5. The data acquisition system used to evaluate imaging parameters.

Due to the properties of this type of low cost camera, imaging noise from the camera can be significant. In order to reduce this image noise, we can designate an average of successive frames or an integration of successive frames for better dynamic range in the final data.

A number of variables, such as the intensity of the illumination light, the angle of the incident light, the type of source used, and the effects of the ambient light, are important to control as they affect the image quality significantly. For example, we varied the angle of incidence of the illumination light and found that significant variations occurred over a range of 30 degrees. Figure 6 shows the results over the first 15 degrees. Increasing the angle of incidence over 25 degree produced little effect. This change in the image contrast is important as it controls the robustness of the feature extraction methods. Figure 7 shows the effect of the ambient lighting. The trend in the signal is a result of the illumination from the sample and the surrounding apparatus. This introduced a significant influence on the images as the part is scanned. This varying effect on the ambient light lead to the design of the data acquisition system that uses the same pixel elements in the camera and allows for the uniform illumination of the surface. As noted (12) the pixel to pixel variation in the CCD camera produce a noise like structure in the image. By using only one row of pixels in

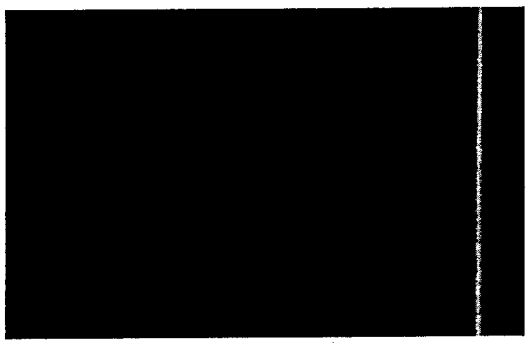

10 degrees

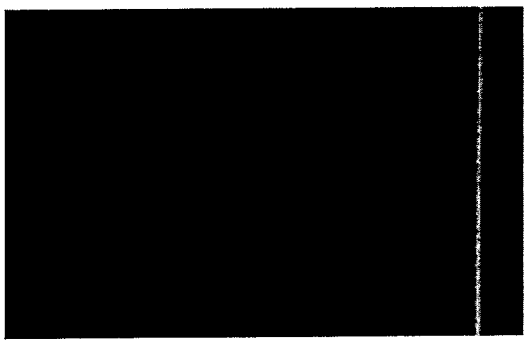

15 degrees

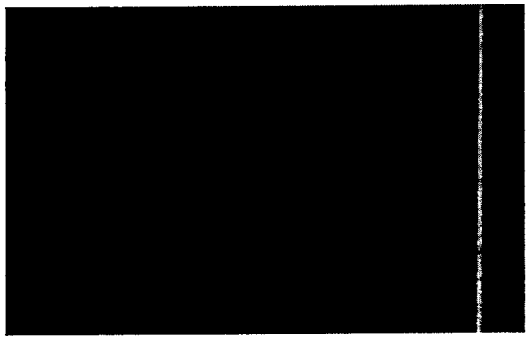

20 degrees

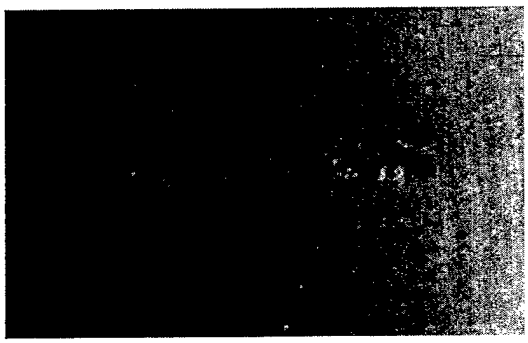

25 degrees

Figure 6. Images taken with the angle of incidence ranging from 10 to 25 degrees. The increase in the contrast in the image is apparent in comparing the 10-degree image with the 25-degree image.

the image acquisition coupled with the scanning of the sample under the objective, we maintain a constant ambient light and use the same pixel elements from the camera, thus eliminating the variability in the images due to these parameters. The result is a simplification of the trend removal necessary as a preprocessing step for the feature extraction.

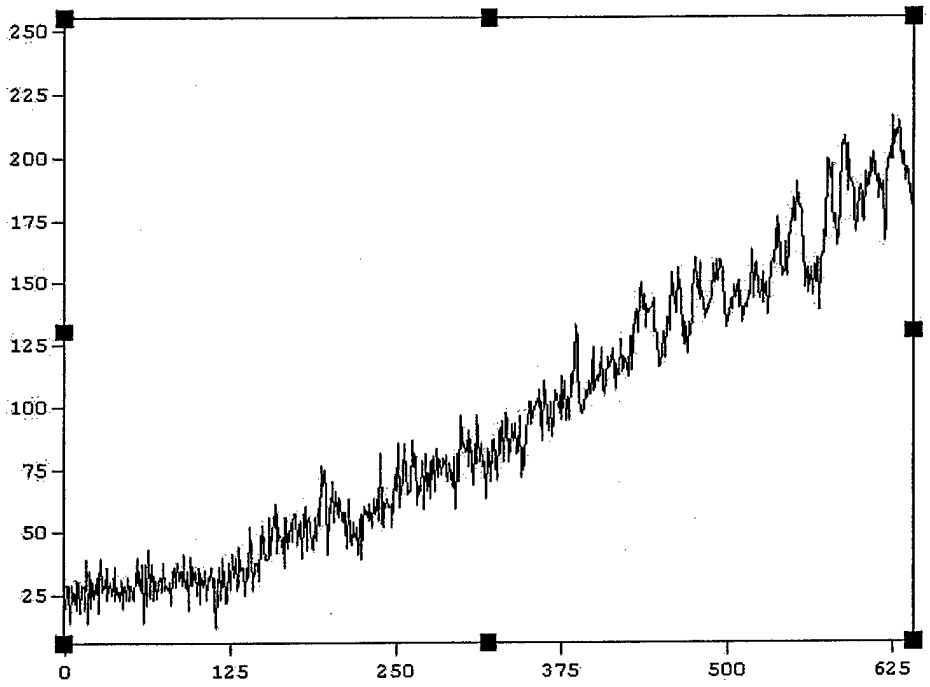

Figure 7. This plot shows the effect of the ambient lighting in the generation of a trend in the intensity of the light. The trend increases to the right; the fluctuation in the signal is the noise. In an ideal system this plot should show a flat plot with the average signal at 25.

The basic approach of the image acquisition system is based on forming 2D images from line scans as the part passes by. The camera and the light source are fixed and they always point at the same direction. The lighting condition does not change with the time or with the movement of the samples. When a 2D image is taken, one of the 640 columns or one of the 480 rows in the image is selected through user interface. This row is saved and the 2D image is built up as the sample is moved step by step. This action is repeated for as many steps as desired. At the end of the scanning, a new 2D image is formed. Each of these line scans has exactly the same background light intensity gradient and CCD systematic noise. As a result, the final image will have a one-dimensional lighting gradient that is uniform throughout the image. This becomes important in developing an image feature extraction algorithm.

We have employed three different light sources for the experiments. The first source had a special fiber probe that could illuminate the target area internally through the boroscope. The second source was a white spectrum light source that has been used to illuminate the target area externally. The third source was a laser light source that illuminated the target area externally.

In this project, we investigated both specular reflections, figure 9, and diffuse reflection, figure 6, for fretting flaw characterization. Due to the glare and very large background light gradient, the diffuse light reflection implementations were not found to

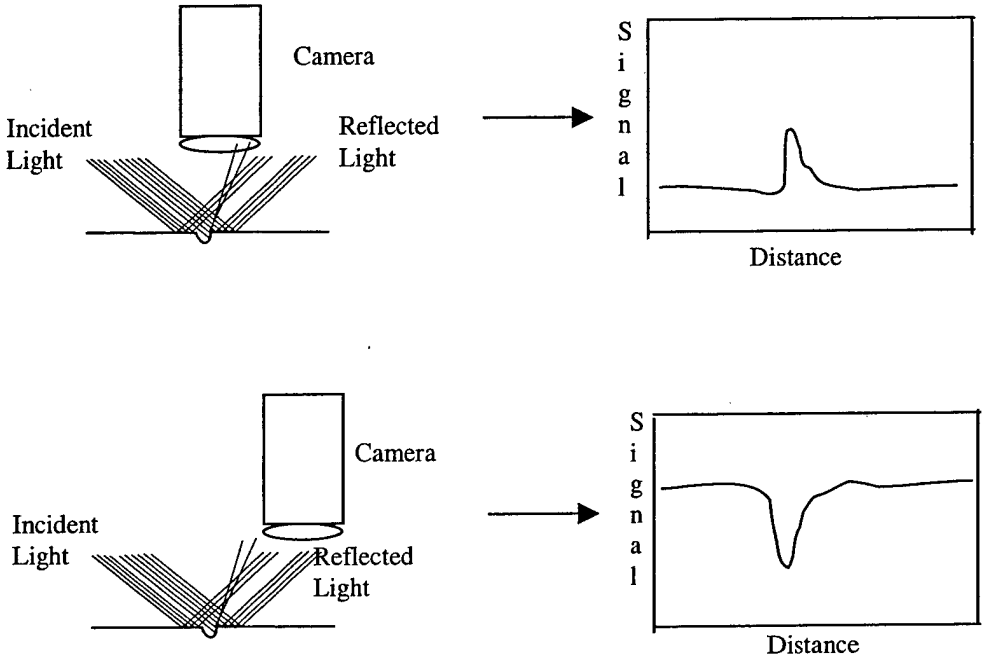

Figure 8. Dark field specular reflection (top) and light field specular reflection (bottom) signal formation cases.

be very promising. Although glare problem can be reduced with light polarizers, we did not push for the diffuse reflection further.

The specular reflection refers to reflection cases where the light incidence angle is basically the same as the angle between the reflected light and the surface. The specular reflection is usually used for characterizing surface defects on flat objects. One requirement for specular reflection approach is to employ a structured light source. In our implementation, we used a laser light source for the specular reflection approach. Depending upon the configuration of the system, the specular reflection is either a dark or light field reflection case. If the reflected light is allowed to reach the camera, this is a light field implementation. Any dark spots in the image will point out surface defects for this case. In contrast with this, the dark field implementations configure camera to receive light reflected from the surface flaws. Figure 8 presents schematic diagrams dark and light field specular reflection image formations. The incidence angle of the light plays an important part in specular reflection implementations. If the light beam is a

well-collimated light beam, the signature of the surface flaw should change with the light incidence angle. We have used this property for flaw surface area and flaw depth estimation.

The first set of results is a dark field case. In this case, the laser light incidence angle has been increased from 20 degrees to 50 degrees with 5-degree increments. As the incidence angle increase, the light reflected from the sample background enters into the camera resulting in a reduction in contrast between the surface flaw and the background. The actual dimensions of the surface flaw are 0.24 mm. width and 2.7 mm. length. The boroscope is about 5 mm from the sample surface. The pixel sizes on the images are 15μm *x* 12μm. The images are made up of 640*x*200 pixels.

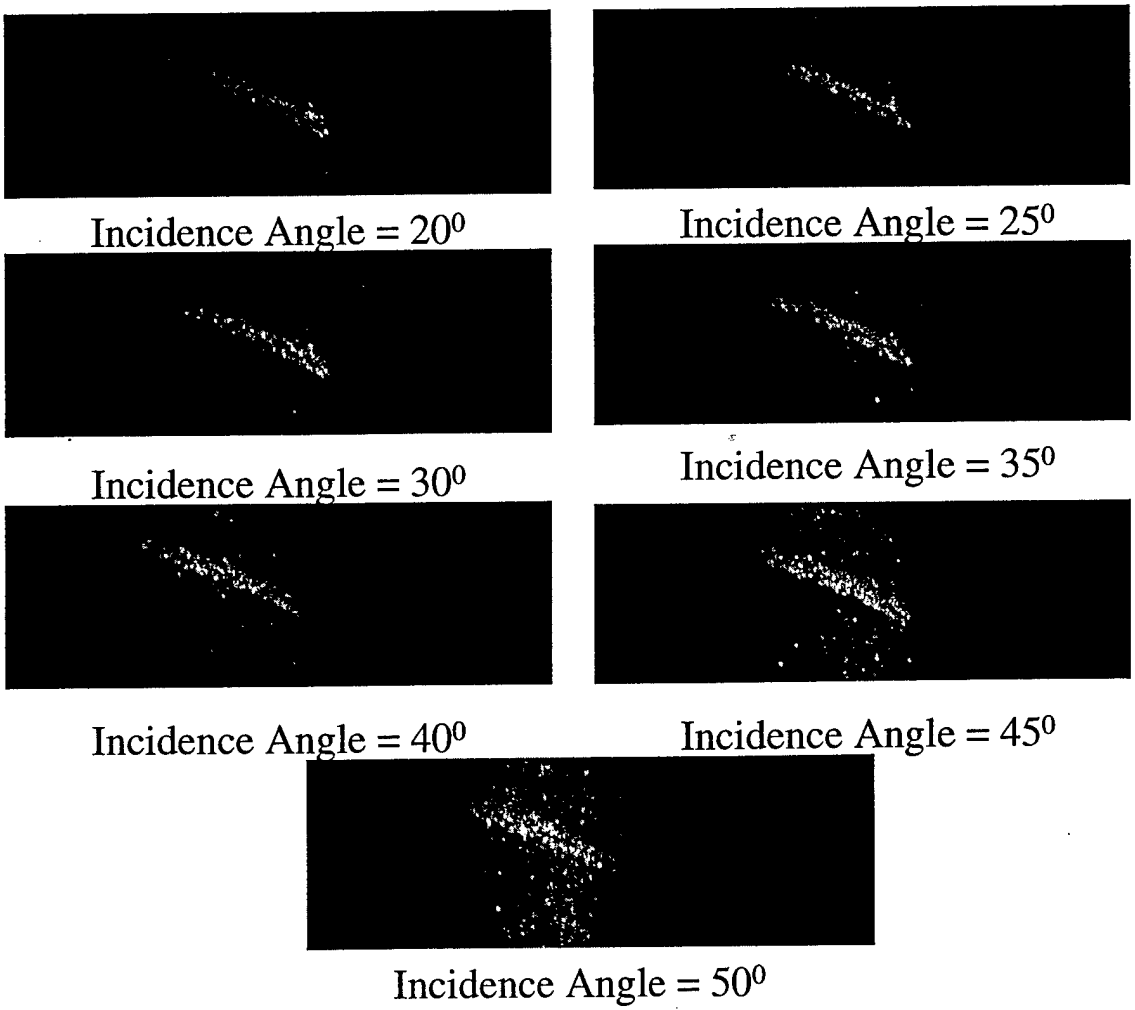

Figure 9 A series of dark field images using the laser source and specular reflection. The incident angle was varied over a range of angles from 20 degrees to 50 degrees.

As can be seen in these seven images, the increase in the incidence angle increases signal intensity from the surface flaw. Once the incidence angle passes 40^0, the background starts to contribute some to the signal coming from the flaw. In order to show the change in the signal intensity with the incidence angle, we plot the gray scale histogram from images produced light having 20^0 and 50^0 incident angles. As it will be seen in Figure 10, the gray scale histogram shifts significantly to the right, a result of the increasing background contribution to the light reaching the camera. In addition to evaluating changes in the shape of the histogram of the images, we also examined the signal intensity by using a threshold where pixel values were converted into a binary scale by applying a threshold value. When the value is below a set threshold, that value was changed to 0, it was changed to 1 if it was above the threshold. Following this, we employed a filter where the small windows of the image were converted to either 1 or 0 if the density of the window was below or above a set density level. By counting the number of pixels in the threshold image with a value of zero we obtain a measure of the flaw area. We plot the flaw area as a function of the incidence angle to show that incidence angle can provide information regarding the flaw area. Figure 11 displays variation of the flaw area as a function of the incidence angle.

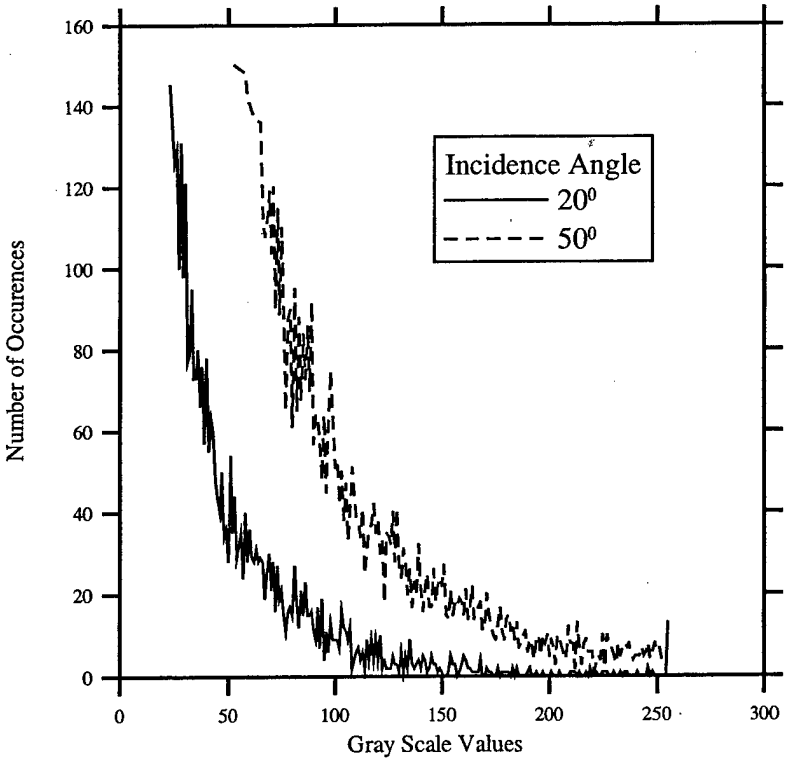

Figure 10. Gray scale values histogram for two incidence angle cases

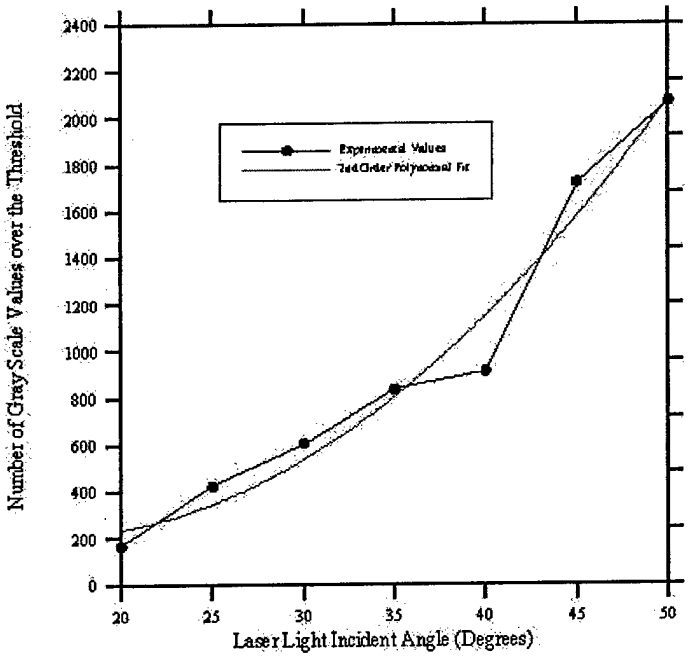

Figure 11. The increasing signal as measured from the thresholded image as a function of angle is shown.

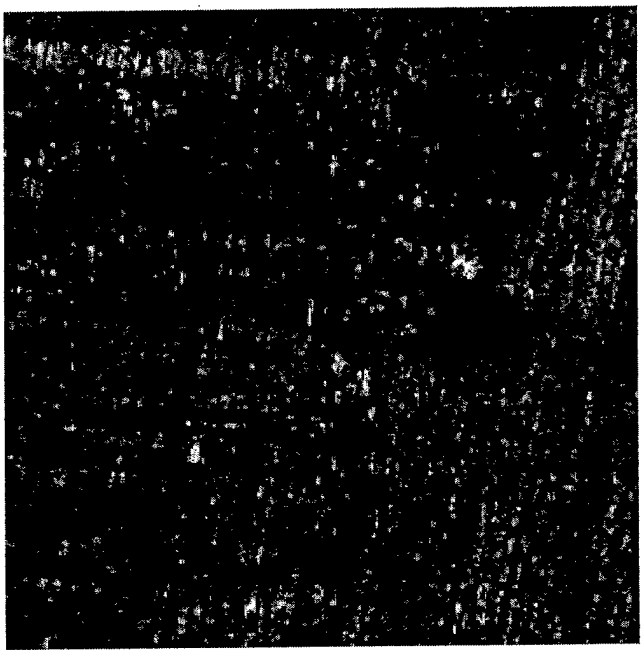

Figure 12. 50x optical microscope image of the area flaw in case II.

The second set of images is an example of light field specular reflection technique. In this case, the flaw is not a scratch but an area flaw that was formed through mechanical means. Its depth varies between 1-7μm. An optical microscope image of this flaw with 50x magnification is given in Figure 8. For this case, we used incidence angles from 8^0 to 25^0. These raw images are given for 8,11,16,20,22 and 25^0 incidence angles.

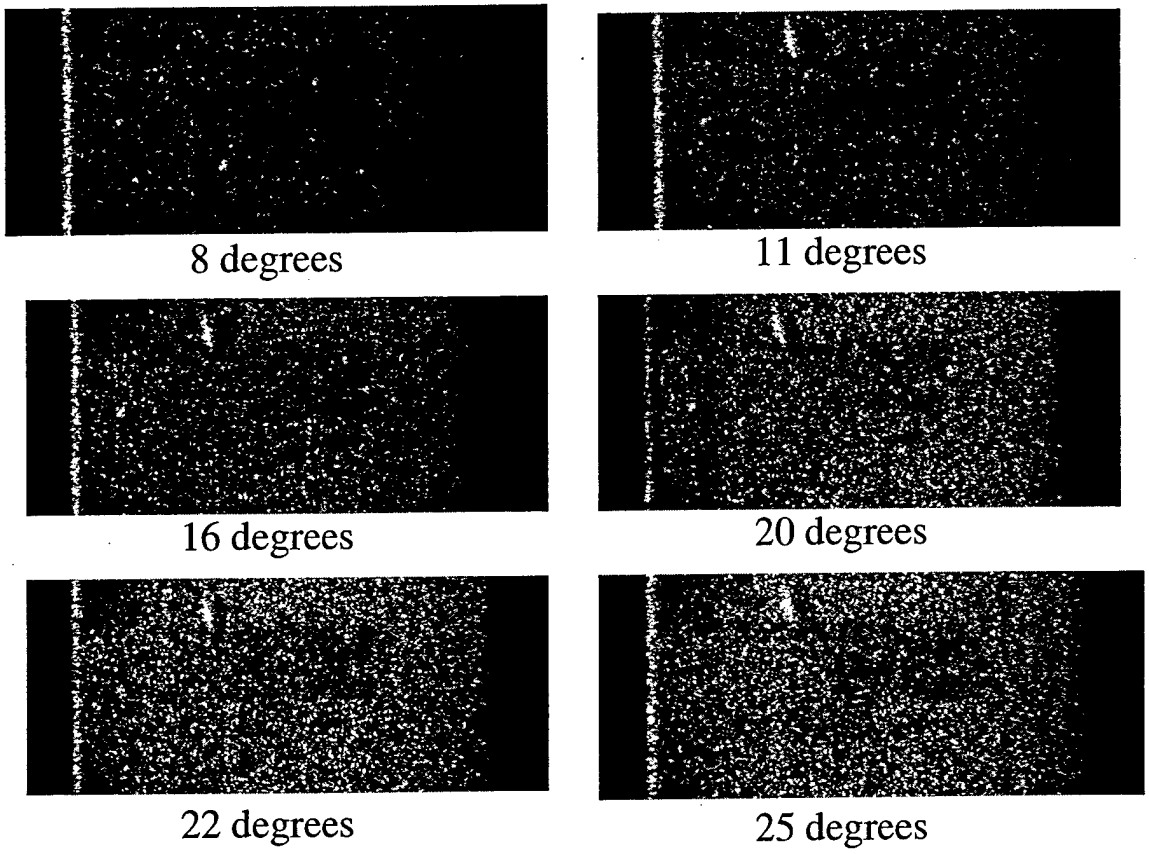

Figure 13. Images of the sample fretting mark showing the effect of the angle of illumination using specular reflections.

We employed a simple threshold filtering with this set of images as well. These processed images are shown below in the same sequence as above. The processed images make it very clear that as the incidence angle increases the dark areas shrink. As the angle of the illuminating light changes, it reflects off deeper areas of the surface features.

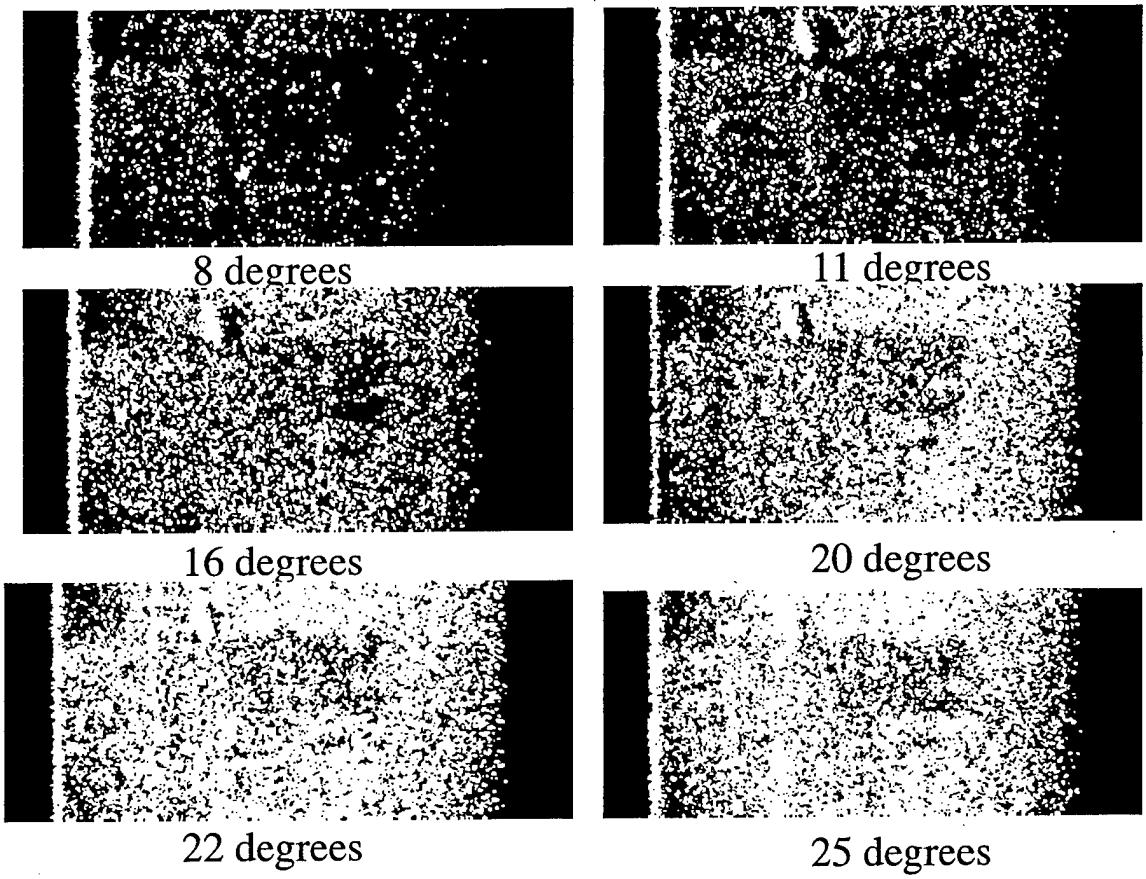

Figure 14. The result of the threshold technique described above on the images generated from specular reflections. The dark portion of the image, especially for the fretting area, decreases as the angle of incidence increases. The increasing incident angle causes deeper portions of the surface feature to be illuminated.

Feature Extraction

The optical images of aircraft turbine disks with and without fretting damage clearly indicate that fretting damage regions have a distinctive grain pattern or texture as shown in Figure 15-a. The image of disks with fretting damage appear elongated along certain orientation while disks with out damage have randomly oriented grains. This distinct feature has been exploited for fretting damage detection and characterization. The overall image analysis task is divided into 3 steps:

1. Segmentation - separates the inspected areas from background.
2. Boundary Extraction- extracts the outlines of regions containing fretting damage.
3. Characterization - derives a quantitative measure of the damage.

1. Image Segmentation

The images of aircraft turbine disks contain objects at several scales including small scale objects such as noise, medium scale structures such as ridges due to fretting damage and large scale structures such as blade slot edges. In order to enhance the small scale structures in the image, morphological filters are used. Morphological operations are composed of two elementary operations namely dilation and erosion. The underlying idea in morphological filtering is detection of features using a structuring element derived from a priori knowledge of the image. In this analysis, the structuring element used is a square of size 3X3. The structuring element size is crucial and is selected based on the width of ridges and grooves in the damaged regions. Image scales smaller than the structuring element are detected from the residual image, which is the difference between the original image and filtered version obtained by applying the morphological operator to the image. Figure 15-b shows the results of morphological filtering on the engine disk image with fretting damage shown in Figure 15-a. As seen in the result, the background image containing the blade slot edges is de-emphasized and the ridges and grooves associated with fretting damage are enhanced.

2. Boundary Extraction

Once fretting damage regions have been detected, fine detail analysis is employed locally for fretting damage characterization. A boundary extraction algorithm is used for estimating the location and spatial extent of the damaged region and also providing geometrical detail of the region. The algorithm is implemented based on a vector image model and particle motion in a vector field. Figure 16 illustrates the result of boundary extraction: Figures 16-a shows the enlarged view of fretting damage area in Figure 15-a, Figure 16-b shows the results of morphological processing, and Figure 16-c shows the extracted boundaries. Figure 17 shows another example of the fretting damage image and the extracted outlines. Note that, in Figure 17, fretting damage is contained in the diagonal area of the image. The distinctive elongated shape of the ridges associated with fretting damage is clearly visible.

3. Characterization

Several approaches are possible for characterizing the fretting damage. The processed image after steps 1 and 2 can be used to determine quantitatively the size of the grains. A statistical analysis of the grain size distribution could be correlated with the extent of the damage. Such studies will require the availability of a sufficiently large set of measurements from disk slots.

Other possible approaches include estimation of the depth map from 'shading' effects in the original image with respect to illumination angle and retrieval of depth using stereoscopic (left and right) optical images of the slot region. However all these algorithms require availability of significant amount of additional data.

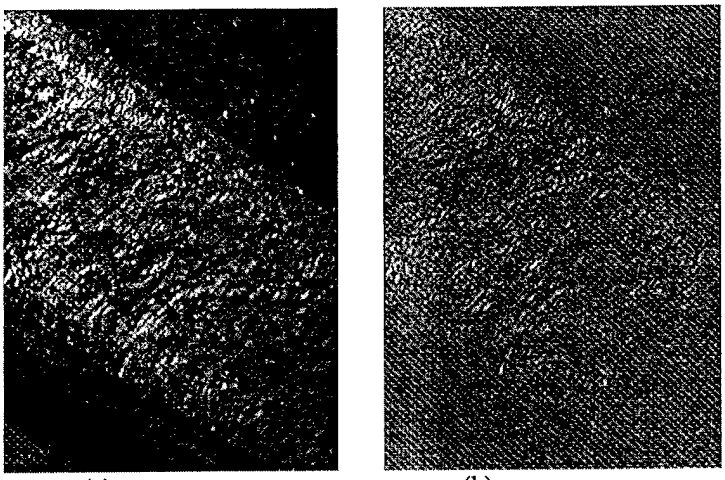

(a) (b)

Figure 15: (a) Image of engine disk with fretting damage; (b) image after morphological filtering.

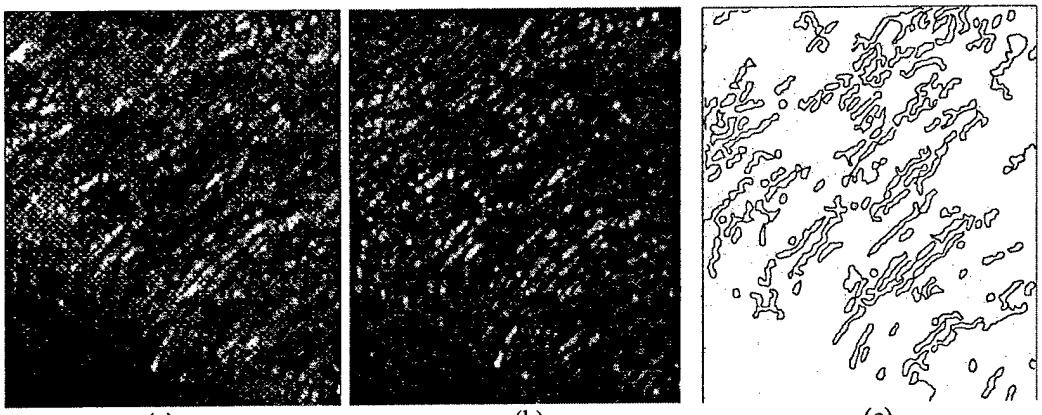

(a) (b) (c)

Figure 16: (a) Enlarged area of fretting damage; (b) image after morphological filtering; (c) boundary extraction result.

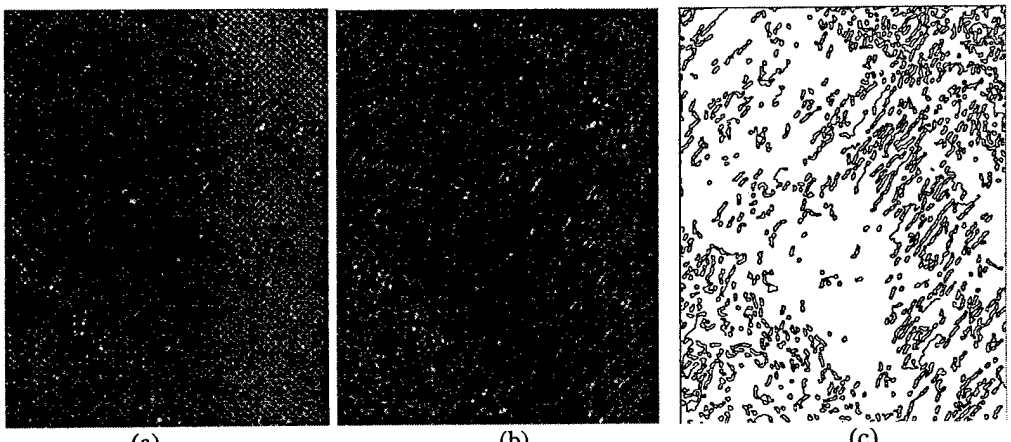

(a) (b) (c)

Figure 17: (a) Fretting damage image; (b) image after morphological filtering; (c) boundary extraction result.

Conclusions

The first key issue that quickly became apparent as this project began was the need for uniform, controlled illumination conditions. The results shown require stationary backgrounds and most importantly require that as the probe is scanned over tha part that the brightness of a particular feature be constant. Over rough surfaces, whether from a natural sufrace finish or from an abraded feature, the brightness from a wide angle of illumination resulted in different intensities being reflected from the same areas of the part over the course of the scan. While features for a particualr illumianation were easily analysed, the variability as a scan progressed made quantitative analysis impossible. This lead to a series of experiments directed at identifying and subsequently controlling the variability.

Several sources for this variability were identified, including the effects of the camera responses, the type of illumination, the ambient room illumination and the angle of the incident light. In order to address this issues we developed a data acquisition method that significantly reduced the magnitude of the ambient light and cammera artifacts. Several of the important issues from the camera include the imperfect pixel to pixel response. In an ideal camera with a uniform illumination, the result would be a constant valued image. This is not the case. The addition of the variable ambient lighting resulting from the scan postion changing along the surface exacerbated this effect. By using a single row of camera pixels and scanning the surface much like a x-ray baggage scanner, we were able to eliminate much of the signal variability. The results of the illiminatiion angle could now be systamaticly studied. The results illustrated in figures 13 and 14 show the reproducibility of the images and the much more tractable uniform backgrounds.

While the results showing sensitivity to both area and depth are suggestive, further work will be required to determine the level of accuracy that the methods can achieve. One of the goals was to demonstrate a means using equipment that would by adaptable to field conditions, as opposed to laboratory conditions. The depth sensitivity demonstrated in firgure 14 was shown for a few microns. The depth of field technique applied by using a icroscope to measure the height of surface features is time consuming and somwhat exacting. Specifically the resoultion of both the microscope and of the optical surface imaging developed are on the oders of a few microns. Figure 18 shows an example of the depth of field measurments of the surface features height. The issue is one of registry of the relevant region chatacterized wit the microscope to the scanning system.

The demonstration of standard imaging hardware coupled with a novel method of eliminating much of the signal variability we believe meets the initial demonstration that such a technique is feasible. The stabilization fo the data collection to provide a reprducible result ameinable to standrard image processing techniques was a key element of this demonstrations. The morphological processing to identify areas of freatures coupled with the angular sensitivity to very small changes in surface height show that the autimated image acquisition and presentation to an operator are mangable.

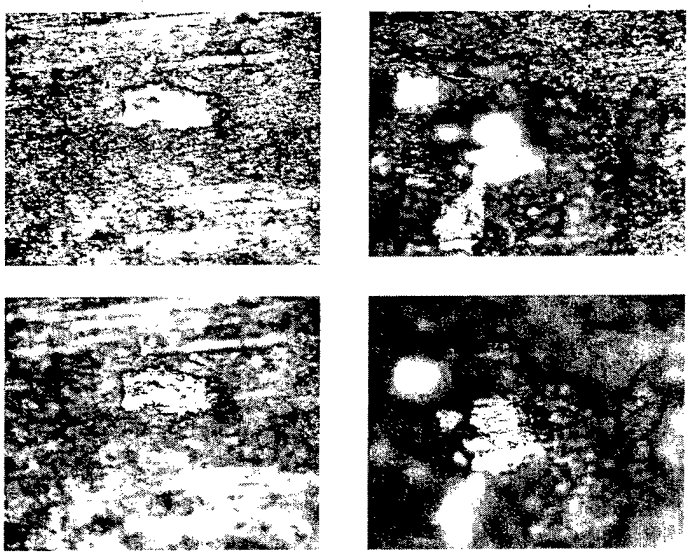

Figure 18 The depth of field of a microscope is used to measure the height of features on a fretted section of a turbine disk. The left pair of images illustrates a feature 3 microns in height. The right pair of images shows a feature 7 microns in height. The ridges reported for in service fretting damage are 50 to 100 microns.

Future Directions

To complete that demonstration of this approach we need to obtain a richer set of samples covering a wide range of fretting. With these samples we would measure the height profiles with microscope field of focus technique and develop a fuller correlation of area and height of the feature from different angles.

References

[1] ASM Handbook: Failure Analysis and Prevention, vol. 11, 1992

[2] E. Doering, J. Basart, J. Gray, " Three-dimensional Flaw Reconstruction and Dimensional Analysis Using a Real Time X-ray Imaging System", NDT&E International, vol. 26, 1, p.7, (1993)

[3] Ed Doering, Ph.D. Thesis, ISU 1993

[4] J. Serra, *Image analysis and mathematical morphology* (Academic Press, London, 1982).

[5] R. A. Peters, "A new algorithm for image noise reduction using mathematical morphology," *IEEE Trans. Image Processing*, vol. 4, no. 5, pp. 554-567, 1995.

[6] R. Lippmann, "An introduction to computing with neural nets," *IEEE ASSP Magazine,* vol. 4, pp. 4-22, 1987.

[7] R. Polikar, L. Udpa, S. S. Udpa, and T. Taylor, "Frequency Invariant Classification of Ultrasonic Weld Inspection Signals," *IEEE Transactions on Ultrasonics, Ferroelectrics and Frequency Control*, Vol. 45, No. 3, pp. 614-625, May 1998.

[8] L. Udpa and S. S. Udpa, "Neural Networks for Classification of Nondestructive Evaluation Signals," *IEE Proceedings F Special Issue on Radar and Signal Processing*, Vol. 138 (1) pp. 41-45, February 1991.

[9] L. Udpa and S. S. Udpa, "Eddy Current Defect Characterization Using Neural Networks", *Materials Evaluation* , Vol. 48, No. 3, pp. 42-347, March 1990.

[10]N. Eua-Anant and L. Udpa, " A Novel Boundary Extraction Algorithm Based on a Vector Image Model", *Proceedings 1996 39th Midwest Symposium on Circuits and Systems,* pp. 597-600, 1996.

[11] N. Eua-anant and L. Udpa, "Boundary detection using simulation of particle motion in a vector image field," *IEEE Transactions on Image Processing*, Nov 1999, pp.1560-1571).

[12] R.Wallingford and J.Gray, "Real Time image Processing; Techniques for Sensitivity Improvement Using Low-cost Equipment", "Review of Progress in Quantitative Nondestructive Evaluation", vol. 14A, p 871, Eds. D. Thompson and D Chimemti, Plenum Press, New York, 1995